Viability of Bianchi-V Universe in $f(R,T)$ with Observational Constraints

Lokesh Kumar Sharma,[1]★ Suresh Parekh,[2] Kalyani C.K. Mehta, [3] Saibal Ray[4] and Anil Kumar Yadav[5]
[1] *GLA University, Mathura 281406, Uttar Pradesh, India*
[2] *Department of Physics, SP Pune University, Pune 411007, Maharastra, India*
[3] *Department of Physics, Eberhard Karls University of Tubingen, Germany*
[4] *Center for Cosmology, Astrophysics and Space Science (CCASS), GLA University, Mathura 281406, Uttar Pradesh, India*
[5] *Department of Physics, United College of Engineering and Research, Greater Noida 201 306, India*

Accepted XXX. Received YYY; in original form ZZZ

ABSTRACT

In this paper, the possibility of a Bianchi-V universe in the gravitational field theory $f(R,T)$ is examined. We constructed a singular Lagrangian model based on the connection between the trace of the energy-momentum tensor T and the Ricci scalar R in order to solve the field equations. The power law for the scaling factor was also considered. . We constrain the model with the Hubble parameter ($H(z)$) dataset, Baryon Acoustic Oscillations (BAO) dataset, Pantheon dataset, joint $H(z)$ + Pantheon dataset, and collective $H(z)$ + BAO + Pantheon dataset. The outcomes for H_0 are as follows: $H_0 = 68.790^{+2.250}_{-2.046}$ km s^{-1} Mpc^{-1}, $H_0 = 69.499^{+2.561}_{-1.863}$ km s^{-1} Mpc^{-1}, $H_0 = 69.102^{+2.453}_{-2.072}$ km s^{-1} Mpc^{-1}, $H_0 = 67.633^{+2.448}_{-2.013}$ km s^{-1} Mpc^{-1}, $H_0 = 68.381^{+2.219}_{-2.032}$ km s^{-1} Mpc^{-1} respectively. We also address Energy Conditions, $Om(z)$ analysis, and cosmographical parameters like Jerk, Lerk, and Snap. Our estimation of H_0 is remarkably consistent with various recent Planck Collaboration studies that utilize the ΛCDM model. Our results show that the proposed model agrees with the observed signatures within a certain range of restrictions.

Key words: MCMC Model, Cosmological Parameters, Observational constraints, Om Diagnostics, Cosmography

1 INTRODUCTION

In 1998,The discovery of an accelerating cosmos and the subsequent development of fluid dark energy (DE) with negative pressure led to a significant advancement in cosmology (1; 2; 3; 4; 5; 6).Numerous cosmological models have been examined to comprehend the characteristics of DE (7; 8; 9; 10; 11).The cosmological constant Λ is the most viable choice for dark energy; yet, it has certain issues with its theoretical implementation (12; 13; 14; 24).Our understanding of dark energy is limited to its phenomenological characteristics, which remain enigmatic and unclear: (i) DE is a cosmic fluid that violates the strong energy condition and has an equation of state parameter. (ii) DE has a lesser clustering property than dark matter (DM) and is uniformly distributed throughout the universe on a cosmological scale. Apart from the ΛCDM model, there is also the XCDM model where the dynamical dark energy is parametrized along the spatial direction, and the ϕCDM model where dynamical dark energy is represented by a scalar field ϕ (16; 17).We note that the XCDM model is confirmed for a considerably larger set of cosmological data, such as growth factor information, BAO distance measurements, and type Ia supernova (SN Ia) apparent magnitude observations. This encourages us to build a Bianchi type I space-time model of the accelerating cosmos.

The $f(R,T)$ theory of gravity, which was put forth by Harko et al.(18) in 2011, expresses the gravitational Lagrangian in terms of the Ricci scalar R and trace T. It is evident that $f(T)$ and matter function as an effective cosmological constant. Therefore, adding a DE component to the $f(R,T)$ theory of gravity may help explain the Universe's late temporal acceleration. Harko has since looked into the thermodynamic consequences of the matter-geometry coupling of generalised gravity models (19).The following are some significant uses of the $f(R,T)$ theory of gravity (20; 21; 22; 23). Nojiri and Odintsov have studied a theoretical cosmological model where $f(R)$ is used in place of the action (24).Observe that the late temporal acceleration of the Universe has been satisfactorily represented by cosmological models motivated by $f(R)$ gravity (25).The authors have looked at feasible cosmological models that meet the requirements of the solar system test for the $f(R)$ theory of gravity(26). We study an anisotropic singular universe model in $f(R,T)$ gravity with nonminimal matter geometry coupling. The field equations have been precisely solved by accounting for the scale factor's power law change, which drives ΛCDM cosmology. It is important to note that the $f(R,T)$ theory plays a significant role in evoking a comprehensive theoretical explanation for the acceleration of the universe at late times without the assistance of unusual matter or energy.

With the help of the presence of dark energy and dark matter, the $f(R,T)$ theory of gravitation contributes significantly to the explanation of the universe's current acceleration. Different models regarding different features of the functional form of $f(R,T)$ gravity have been proposed up to this point (20; 27; 28).According to this hypothesis, the way that various matter components interact with space-time curvature is a cosmological outcome.Nevertheless, a significant contribution of EMC violation causes accelerated expansion in the cosmological models of $f(R,T)$ gravity. The impact of EMC violation in this theory has not yet been thoroughly investigated. A few first investigations of celestial objects using the $f(R,T)$ theory of gravity (29; 30; 31; 32; 33).Inspired by the previous conversation, we now set out to study a cosmological model with nonminimal matter-

★ E-mail: lokesh.sharma@gla.ac.in (KTS)

geometry coupling in Bianchi V space-time with gravity defined as $f(R,T) = f_1(R) + f_2(R)f_3(T)$. It is noteworthy that the cosmological implications of a nonminimal matter-geometry coupling in the $f(R,T)$ theory of gravitation are explored by means of a product between R and T, or functions of them, in this functional form of $f(R,T)$ gravity.The simplest coupling $f_1(R) = f_2(R) = R$ and $f(T) = \zeta T$, with ζ a constant—will be used in this article. Within the $f(R,T)$ gravity formalism, the function f(R; T) has a nontrivial functional form that involves nonminimal matter-geometry coupling. Additionally, it benefits from the fact that $\zeta = 0$ is the retrieval of general relativity. A few practical uses for $f(R,T) = f_1(R)+f_2(R)f_3(T)$ in various physical situations (20; 34)

2 THE BASIC OF $F(R,T)$ THEORY OF GRAVITATION AND SCALE FACTORS

Bianchi V space-time is read as

$$ds^2 = -c^2dt^2 + (C^2dz^2 + B^2dy^2)e^{2\alpha x} + A(t)^2dx^2 \tag{1}$$

Here, A(t), B(t), and C(t) are scale factors along the x, y, and z axes, and α is a constant. The action in f(R, T) gravity is given by

$$S = \frac{1}{16\pi}\int d^4x\sqrt{-g}f(R,T) + \int d^4x\sqrt{-g}L_m, \tag{2}$$

where g and L_m are the metric determinant and matter Lagrangian density, respectively. The gravitational field of $f(R,T)$ gravity is given by

$$\begin{aligned}&[f_1'(R) + f_2'(R)f_3'(T)]R_{ij} - \frac{1}{2}f_1'(R)g_{ij}\\ &+ (g_{ij}\nabla^i\nabla_j - \nabla_i\nabla_j)[f_1'(R) + f_2'(R)f_3'T]\\ &= [8\pi + f_2'(R)f_3'(T)]T_{ij} + f_2(R)\left[f_3'(T)p + \frac{1}{2}f_3(T)\right]g_{ij}.\end{aligned} \tag{3}$$

Here, $f(R,T) = f_1(R) + f_2(R)f_3(T)$ and primes denote derivatives with respect to the arrangement

Following Moraes and Sahoo [4], we assume $f_1(R) = f_2(R) = $ R and $f_3(T) = \zeta$T, with ζ as a constant. Thus, Eq. (3) yields

$$G_{ij} = 8\pi T_{ij}^{(\text{eff})} = 8\pi\left(T_{ij} + T_{ij}^{(\text{ME})}\right), \tag{4}$$

where, $T_{ij}^{(\text{eff})}$, T_{ij} and $T_{ij}^{(\text{ME})}$ represent the effective energy-momentum tensor, matter energy–momentum tensor and extra energy term due to trace of energy–momentum tensor, respectively. The extra energy term is read as

$$T_{ij}^{(\text{ME})} = \frac{\zeta R}{8\pi}\left(T_{ij} + \frac{3\rho - 7p}{2}g_{ij}\right). \tag{5}$$

By applying the Bianchi identities in Eq. (4) yields

$$\nabla^i T_{\text{ij}} = -\frac{\zeta R}{8\pi}\left[\nabla^i(T_{\text{ij}} + pg_{ij}) + \frac{1}{2}g_{\text{ij}}\nabla^i(\rho - 3p)\right]. \tag{6}$$

For the line element (1), the field equation (4) can be written as

$$\frac{\ddot{B}}{B} + \frac{\ddot{C}}{C} + \frac{\dot{B}\dot{C}}{BC} - \frac{\alpha^2}{A^2} = -8\pi p^{(\text{eff}),} \tag{7}$$

$$\frac{\ddot{C}}{C} + \frac{\ddot{A}}{A} + \frac{\dot{A}\dot{C}}{AC} - \frac{\alpha^2}{A^2} = -8\pi p^{(\text{eff})}, \tag{8}$$

$$\frac{\ddot{A}}{A} + \frac{\ddot{B}}{B} + \frac{\dot{A}\dot{B}}{AB} - \frac{\alpha^2}{A^2} = -8\pi p^{(\text{eff}),} \tag{9}$$

$$\frac{\dot{A}\dot{B}}{AB} + \frac{\dot{A}\dot{C}}{AC} + \frac{\dot{C}\dot{A}}{CA} + \frac{3\alpha^2}{A^2} = 8\pi\rho^{(\text{eff}).} \tag{10}$$

Here, $p^{(\text{eff})} = \rho + \rho^{(\text{ME})} = p - \frac{3\zeta}{8\pi}\left(\frac{\ddot{a}}{a} + \frac{\dot{a}^2}{a^2}\right)(3\rho - 7p)$, $p^{(\text{eff})} = p + p^{(\text{ME})} = p + \frac{9\zeta}{8\pi}\left(\frac{\ddot{a}}{a} + \frac{\dot{a}^2}{a^2}\right)(\rho - 3p)$, and a = $(ABC)^{\frac{1}{3}}$ is average scale factor. The above Eqs. (7)–(10) can also be written as

$$\frac{\ddot{(ABC)}}{ABC} = 12\pi\left(\rho^{(\text{eff})} - p^{(\text{eff})}\right). \tag{11}$$

We define Hubble's parameter (H) in connection with the average scale factor as follows:

$$H = \frac{\dot{a}}{a}. \tag{12}$$

Following Sharma et al. [5], we have

$$a = (nDt)^{\frac{1}{n}} \tag{13}$$

where n & D are nonzero positive constants. Solving Eqs. (7)–(9) and (28), we get

$$A(t) = (nDt)^{\frac{1}{n}} \tag{14}$$

$$B(t) = \xi(nDt)^{\frac{1}{n}}\exp\left[\frac{\delta}{D(n-3)}(nDt)^{\frac{n-3}{n}}\right], \tag{15}$$

$$C(t) = \xi^{-1}(nDt)^{\frac{1}{n}}\exp\left[\frac{-\delta}{D(n-3)}(nDt)^{\frac{n-3}{n}}\right]. \tag{16}$$

Here, ξ and δ are constants.

3 OBSERVATIONAL ANALYSIS

3.1 Observational Constraints on Model Parameters

In this part, we confine the model's H_0, α, and β parameters to the redshift range $0 \le z \le 1.965$ using the observable H(z), BAO, and Pantheon datasets. The distribution of the datasets for observational H(z) is shown in 1, and the data points are listed in **??**. The details for BAO and Pantheon are taken from (**?**). Furthermore, the scale factor in relation to redshift is provided by:

$$a = \frac{a_0}{1+z} = \alpha t^{\beta} \tag{17}$$

Where a_0 denotes the present value of the scale factor.

The age of the universe is computed with the following equation.

$$H(z) = -\frac{1}{1+z}\frac{dz}{dt} \tag{18}$$

Putting together equations (17 - 18) and after some manipulation, one can easily obtain the following Hubble's function

$$H(z) = \beta\left(\frac{a_0}{\alpha}\right)^{-\frac{1}{\beta}}(1+z)^{\frac{1}{\beta}} \tag{19}$$

From the equation (19), the Hubble constant's present value is determined as $H_0 = \beta\left(\frac{a_0}{\alpha}\right)^{-\frac{1}{\beta}}$.

Table 1. Parameter values obtained from different datasets after running MCMC and Bayesian analysis.

Parameter	H(z)	BAO	Pantheon	H(z) + Pantheon	H(z) + BAO + Pantheon
H_0	$68.790^{+2.350}_{-2.046}$	$69.499^{+2.561}_{-1.863}$	$69.012^{+2.453}_{-2.072}$	$67.633^{+2.448}_{-2.013}$	$68.381^{+2.219}_{-2.032}$
α	$69.012^{+0.092}_{-0.097}$	$68.992^{+0.095}_{-0.112}$	$68.998^{+0.084}_{-0.078}$	$68.979^{+0.099}_{-0.090}$	$69.005^{+0.110}_{-0.092}$
β	$1.001^{+0.009}_{-0.010}$	$0.998^{+0.008}_{-0.011}$	$1.000^{+0.010}_{-0.011}$	$1.006^{+0.009}_{-0.011}$	$1.003^{+0.009}_{-0.010}$
Age of Universe (Gyr)	14.3430291	14.3599188	14.4902335	14.8743956	14.6678171

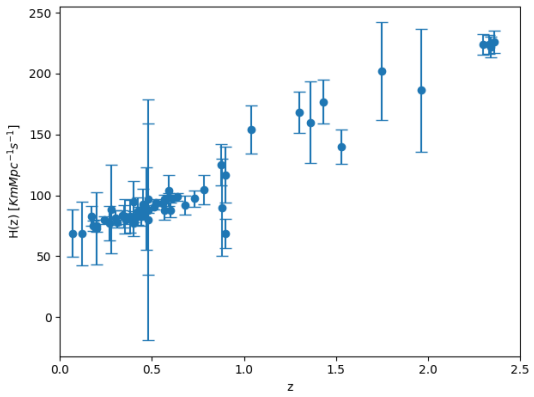

Figure 1. Error bar plot of the 57 point H(z) data used in analysis of our model.

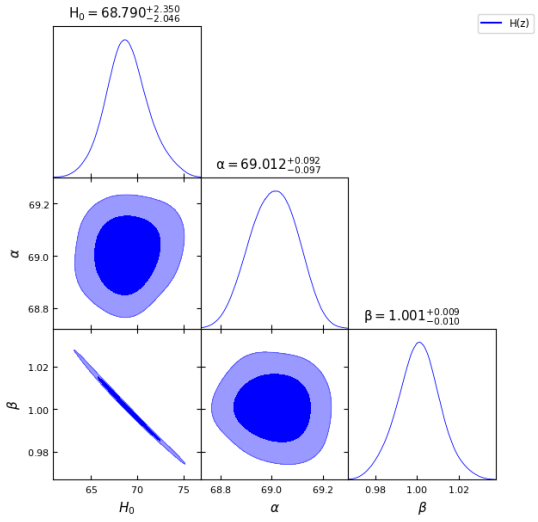

Figure 2. One-dimensional marginalized distribution, and two-dimensional contours for our $f(R,T)$ model parameters H_0, α, β using the H(z) dataset.

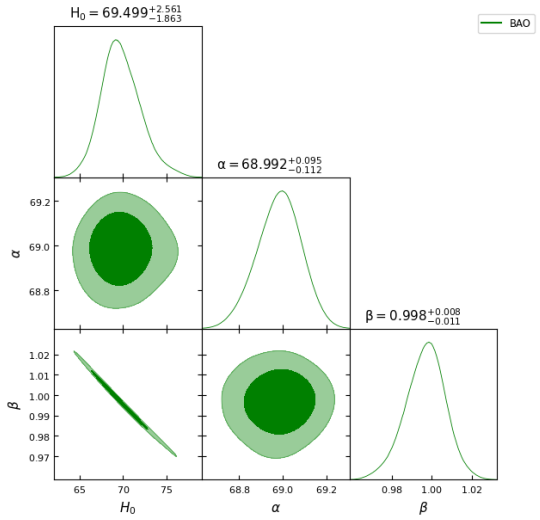

Figure 3. One-dimensional marginalized distribution, and two-dimensional contours for our $f(R,T)$ model parameters H_0, α and β using the BAO dataset.

4 PARAMETERS

4.1 Energy Conditions

Ecs, or energy conditions, analogously establish cosmic laws that elucidate the distribution of matter and energy throughout the cosmos. They emulate the universe's rules and derive from Einstein's gravitational equations. These conditions reveal the distribution of matter and energy in space.

(i) Weak Energy Condition (WEC): According to the WEC, energy can nowhere be negative or zero. This requirement keeps the laws of the cosmos impartial and constant. Using the parameters discovered using the Bayesian Analysis, Figure 16 depicts the WEC's nature for our model.

(ii) Null Energy Condition (NEC): The NEC deals with light. It asserts that energy is a necessary component of all space transit for light and cannot exist in a vacuum. This constraint prevents odd occurrences from occurring and maintains the physics of the cosmos. Figure 13 illustrates the characteristics of NEC for our model utilising the Bayesian Analysis's parameters.

(iii) Strong Energy Condition (SEC): Similar to a more rigid counterpart of the NEC, the SEC. It guarantees that energy cannot be negative and sets boundaries for how objects respond to gravity. "It would be comparable to arguing that gravity can only push something apart." The cosmos benefits from having this rule in place. Figure 15 illustrates the characteristics of SEC for our model utilising the Bayesian Analysis's parameters.

(iv) Dominant Energy Condition (DEC): The DEC expands on the NEC by guaranteeing that energy is not just non-negative but also that its distribution cannot be too volatile. It is comparable to asserting that energy cannot go out of control or travel faster than light. This guarantee prevents the cosmos from presenting any strange surprises. The nature of DEC for our model utilising the Bayesian Analysis parameters is shown in Figure 14.

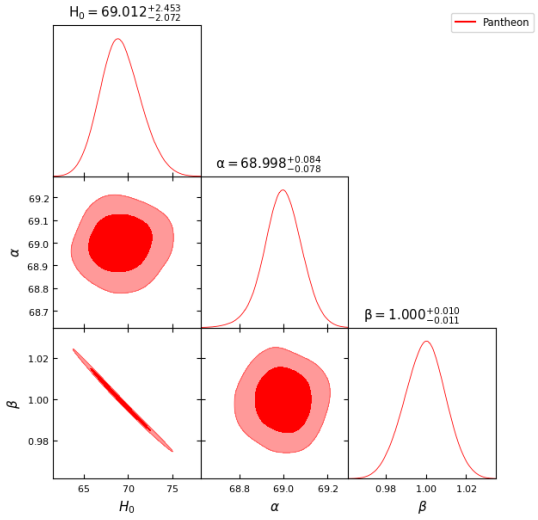

Figure 4. One-dimensional marginalized distribution, and two-dimensional contours for our $f(R,T)$ model parameters H_0, α and β using the Pantheon dataset.

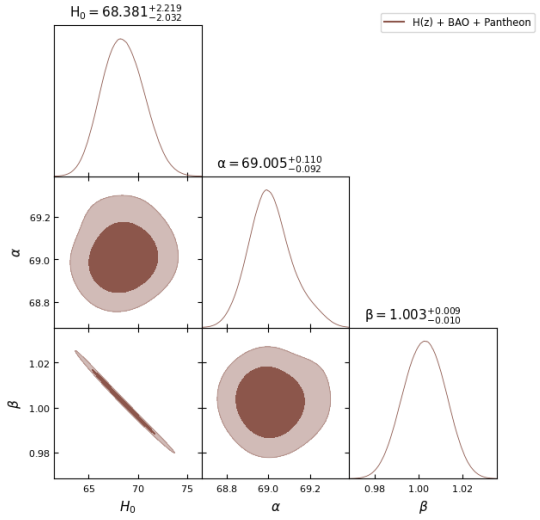

Figure 6. One-dimensional marginalized distribution, and two-dimensional contours for our $f(R,T)$ model parameters H_0, α and β using the combination of H(z), BAO and Pantheon dataset.

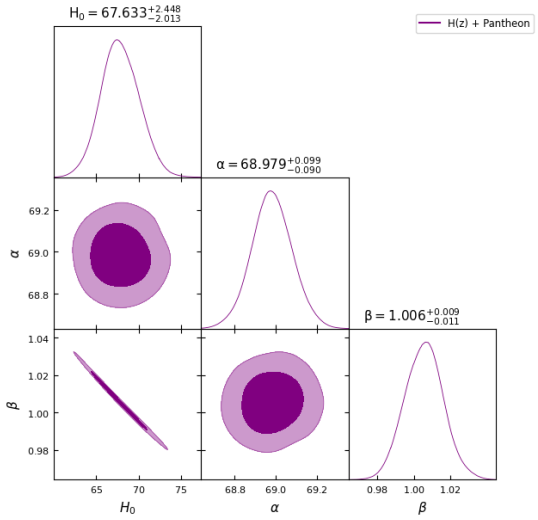

Figure 5. One-dimensional marginalized distribution, and two-dimensional contours for our $f(R,T)$ model parameters H_0, α and β using the combination of H(z) and Pantheon dataset.

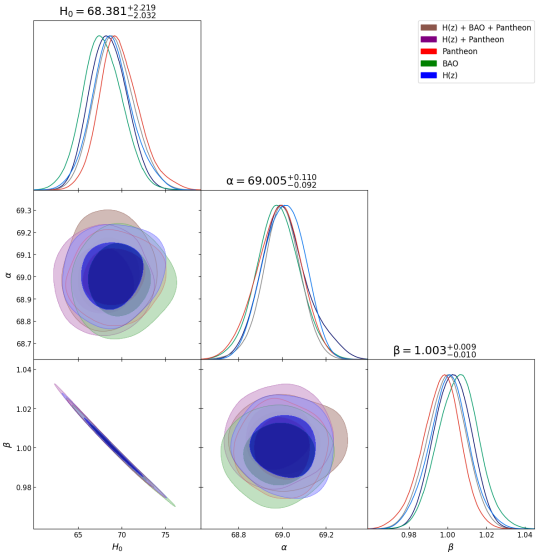

Figure 7. One-dimensional marginalized distributions and two-dimensional contours representing our $f(R,T)$ model parameters H_0, α and β, depicting the combined variability across all dataset combinations.

All energy conditions combined are as shown in the Figure 9 The energy condition relations are as shown below:

$$\text{WEC} \iff \rho \geq 0 \tag{20}$$
$$\text{NEC} \iff \rho - p \geq 0 \tag{21}$$
$$\text{DEC} \iff \rho + p \geq 0 \tag{22}$$
$$\text{SEC} \iff \rho + 3p \geq 0 \tag{23}$$

Figure 10 displays the distribution of energy density *rho* with respect to time t, while Figure 11 displays the distribution of pressure. Our results demonstrate that, except for Strong Ecs (SEC), Null Ecs (NEC), Weak Ecs (WEC), and Dominant Ecs (DEC) are all fulfilled. The universe's rapid expansion justifies the SEC violation. The f (R, T) theory of gravity, which benefits from the contribution of trace energy T, may thus explain the late-time acceleration of the present world without the need for the cosmological constant or dark energy in the universe's energy content.

4.2 State Finder Diagnotics

State Finder Diagnostics are like cosmic detectives who assist us in solving the puzzles of dark energy and the history of the cosmos. These diagnostics guide us through cosmic evolution's complexity as we use a cosmic compass. State Finder Diagnostics are based on the r and s parameters. We can better comprehend the evolution of the cosmos by using these factors. Consider them as cosmic metres that provide information on the expansion of the universe and the elements that make it up. They are dimensionless parameters that capture the essence of cosmic evolution and act as

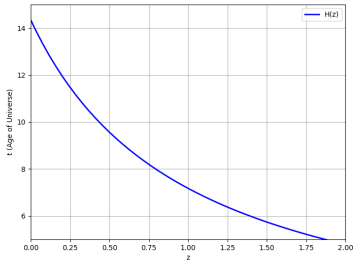

(a)

[htbp]

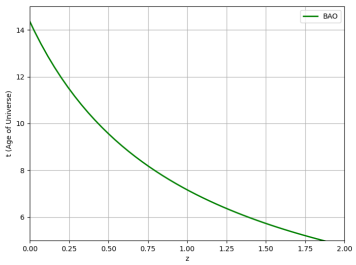

(b)

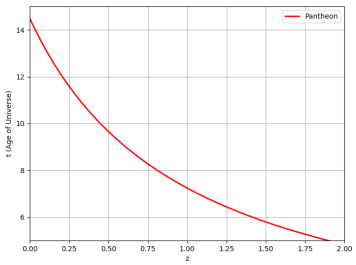

(c)

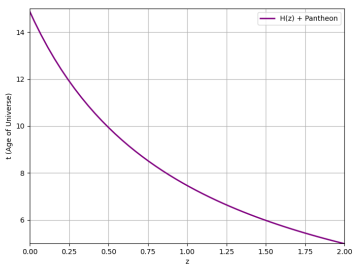

(d)

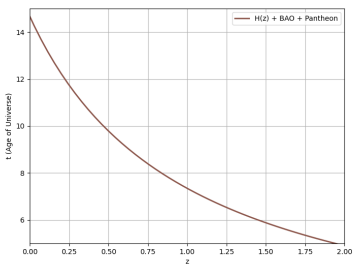

(e)

Figure 8. Graphical representation of cosmic age over redshift. It is crucial for understanding cosmic evolution and validating cosmological models. Five plots are for different combinations of H(z), BAO, and Pantheon datasets. The Age of Universe at z = 0 is mentioned in Table 1.

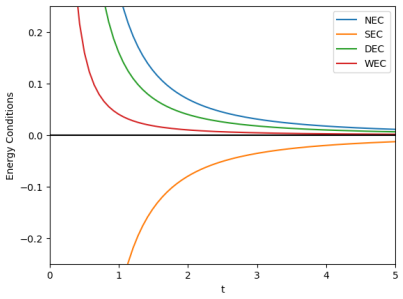

Figure 9. Visualisation of all Energy Conditions vs time.

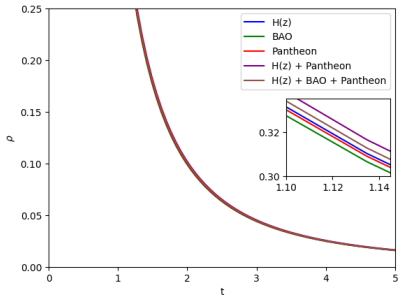

Figure 10. Graphical representation illustrates the dynamic variation of Energy Density (ρ) over time (t) under various parameter conditions derived from distinct combinations of the H(z), BAO, and Pantheon datasets.

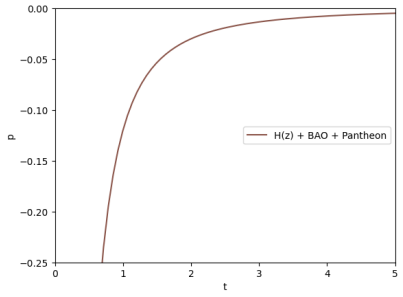

Figure 11. Graphical representation illustrates the dynamic variation of Pressure p over time (t) under various parameter conditions derived from distinct combinations of the H(z), BAO, and Pantheon datasets.

a filter to help us understand the fundamental dynamics of the cosmos. The definitions of their mathematical parameters are as follows:

$$r = \frac{\ddot{a}}{aH^3} \tag{24}$$

$$r = \frac{(-1+r)}{3(-\frac{1}{2}+q)} \tag{25}$$

The equations for r and s in our model, expressed in terms of q, are as follows:

$$r = q(1+2q) \tag{26}$$

$$s = \frac{2}{3}(q+1) \tag{27}$$

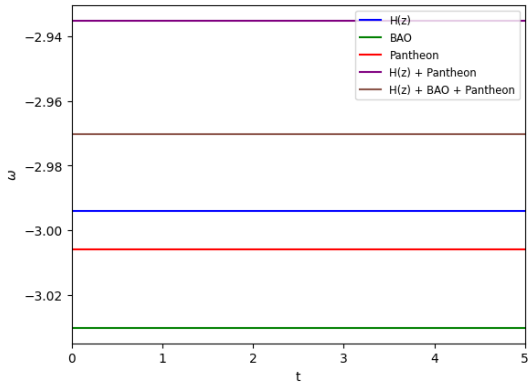

Figure 12. Plot of variation of Equation of state parameter ω v/s time t. The plot suggests that dark energy contributes to the universe's accelerated expansion but with some variations over time, potentially leading to interesting cosmological consequences.

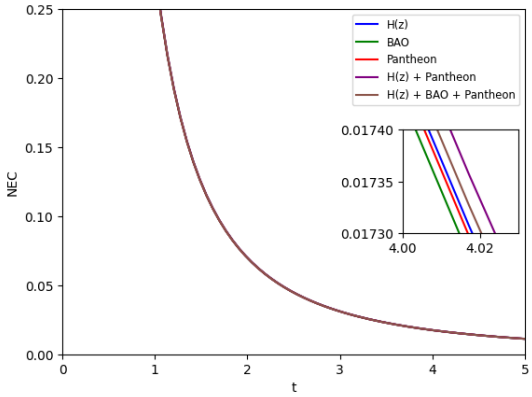

Figure 13. Visualisation of Null Energy Conditions (NEC) vs. time for all dataset combinations.

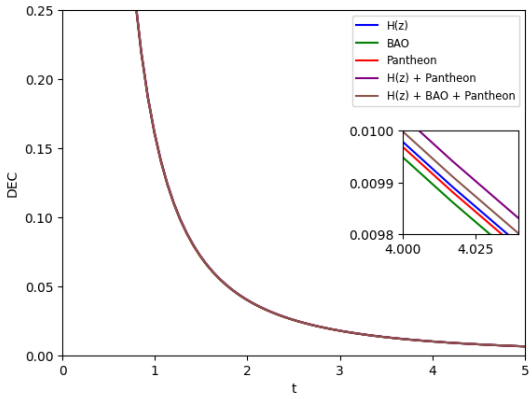

[htbp]

Figure 14. Visualisation of Dominant Energy Conditions (DEC) vs. time for all dataset combinations.

The scale factor trajectories in the resulting model may be shown in Figure 17 to follow a specific set of paths. Our strategy is consistent with the results for the cosmic diagnostic pair from power law cosmology.

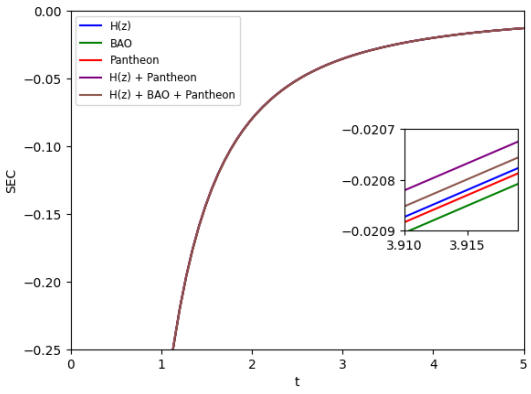

[htbp]

Figure 15. Visualisation of Strong Energy Conditions (SEC) vs. time for all dataset combinations.

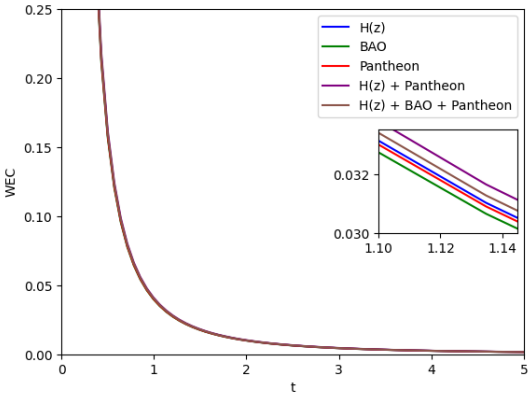

[htbp]

Figure 16. Visualisation of Weak Energy Conditions (WEC) vs. time for all dataset combinations.

4.3 Om(z) parameter

Researchers frequently employ the state finder parameters r - s and the Om diagnostic when analysing various dark energy ideas in academic works. The Om(z) parameter, which is crucial, is created when the Hubble parameter H and the cosmic redshift z merge. Sahoo et al. (2018) present the Om(z) parameter formula in altered gravity.

$$Om(z) = \frac{[\frac{H(z)}{H_0}]^2 - 1}{(1+z)^3 - 1} \tag{28}$$

The Hubble parameter is shown by H_0 in this case. Shahalam et al. (2015) claim that the negative, zero, and positive values of Om(z), respectively, represent the quintessence ($omega \geq -1$), $Lambda$CDM, and phantom ($omega \leq -1$) dark energy (DE) theories. For the current model, we get to the Om(z) parameter as follows:

$$Om(z) = \frac{(1+z)^{2/b} - 1}{(1+z)^3 - 1} \tag{29}$$

4.4 Jerk Parameter

The Hubble and deceleration parameters have received much attention, but the jerk parameter is a little-known treasure that provides

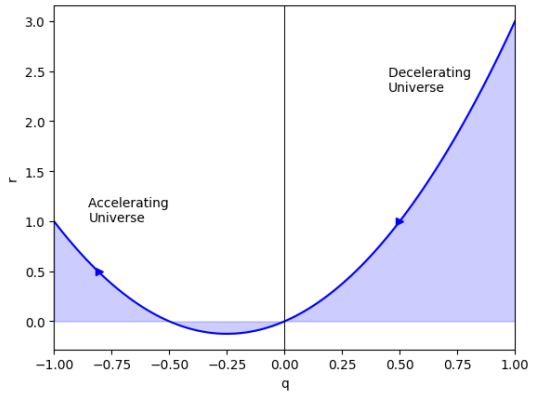

(a)

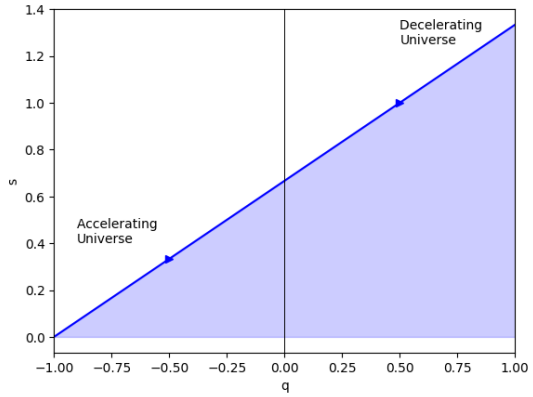

(b)

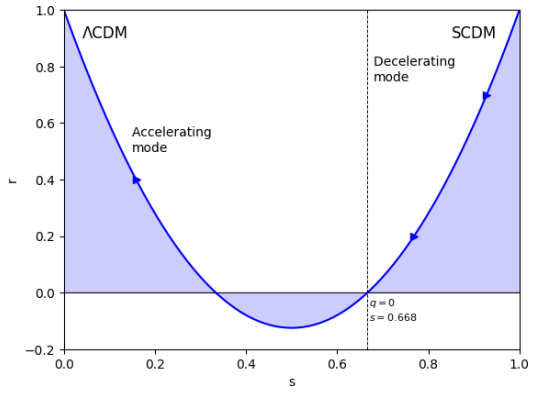

(c)

Figure 17. State Finder Plots of r-q, s-q and r-q.

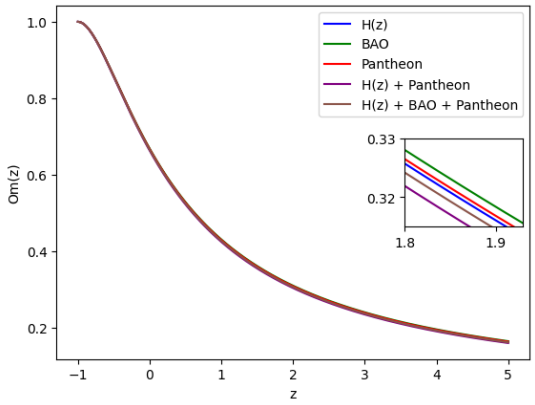

Figure 18. Examining the variations of Om(z) with z across different dataset combinations, considering the β values obtained from each dataset.

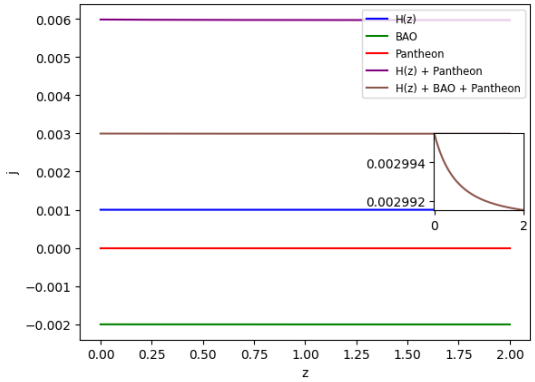

Figure 19. Visualisation of Jerk parameter j v/s z. Values of Jerk parameter at z = 0 are, for H(z) = 0.0009995 s^{-3}, for BAO = -0.002002 s^{-3}, for Pantheon = 0.0 s^{-3}, for H(z) + Pantheon = 0.0059817 s^{-3} and for H(z) + BAO + Pantheon = 0.0029954 s^{-3}

deeper insights into the universe's history. The universe's acceleration is tracked throughout time by the jerk parameter, indicated by the symbol j. The universe's acceleration is accelerating—it is speeding up—when j is positive ($jge0$). The acceleration is said to slow down if j is negative ($jle0$). Different dark energy theories forecast various jerk parameter values. Scientists can learn more about dark energy, the enigmatic factor responsible for the universe's acceleration, by measuring j and comparing it to these predictions. The jerk parameter contributes to the improvement of our models of the cosmos when paired with other cosmic factors. It puts these models to a rigorous examination to ensure they truly reflect what we see in the physical cosmos. Figure 19 depicts the fluctuation of j with respect to redshift z for our model and the derived parameters.

A. G. Riess *et al.* [Supernova Search Team],"Observational evidence from supernovae for an accelerating universe and a cosmological constant,"Astron. J. **116**, 1009-1038 (1998)

A. G. Riess *et al.* [Supernova Search Team],"Type Ia supernova discoveries at z > 1 from the Hubble Space Telescope: Evidence for past deceleration and constraints on dark energy evolution,"Astrophys. J. **607**, 665-687 (2004)

M. Tegmark *et al.* [SDSS],"Cosmological parameters from SDSS and WMAP,"Phys. Rev. D **69**, 103501 (2004)

E. Calabrese, M. Migliaccio, L. Pagano, G. De Troia, A. Melchiorri and P. Natoli,"Cosmological constraints on the matter equation of state,"Phys. Rev. D **80**, 063539 (2009)

Y. Wang and M. Dai,"Exploring uncertainties in dark energy constraints using current observational data with Planck 2015 distance priors,"Phys. Rev. D **94**, no.8, 083521 (2016)

M. M. Zhao, D. Z. He, J. F. Zhang and X. Zhang, "Search for sterile neutrinos in holographic dark energy cosmology: Reconciling Planck observation with the local measurement of the Hubble constant,"Phys. Rev. D **96**, no.4, 043520 (2017)

B. Wang, E. Abdalla, F. Atrio-Barandela and D. Pavon, "Dark Matter and Dark Energy Interactions: Theoretical Challenges, Cosmological Implications and Observational Signatures,"Rept. Prog. Phys. **79**, no.9, 096901 (2016)

P. J. E. Peebles and B. Ratra,"The Cosmological Constant and Dark Energy,"Rev. Mod. Phys. **75**, 559-606 (2003)

T. Padmanabhan,"Cosmological constant: The Weight of the vacuum,"Phys. Rept. **380**, 235-320 (2003)

E. Abdalla and A. Marins,"The Dark Sector Cosmology,"Int. J. Mod. Phys. D **29**, no.14, 2030014 (2020)

M. Li, X. D. Li, S. Wang and Y. Wang,"Dark Energy: A Brief Review,"Front. Phys. (Beijing) **8**, 828-846 (2013)

V. Sahni,"The Cosmological constant problem and quintessence,"Class. Quant. Grav. **19**, 3435-3448 (2002)

J. Garriga and A. Vilenkin,"Solutions to the cosmological constant problems,"Phys. Rev. D **64**, 023517 (2001)

J. Frieman, M. Turner and D. Huterer,"Dark Energy and the Accelerating Universe,"Ann. Rev. Astron. Astrophys. **46**, 385-432 (2008)

S. Nojiri and S. D. Odintsov,"Unified cosmic history in modified gravity: from F(R) theory to Lorentz non-invariant models," Phys. Rept. **505**, 59-144 (2011)

L. Samushia and B. Ratra,"Constraining dark energy with gamma-ray bursts,"Astrophys. J. **714**, 1347-1354 (2010)

M. Yashar, B. Bozek, A. Abrahamse, A. Albrecht and M. Barnard,"Exploring Parameter Constraints on Quintessential Dark Energy: the Inverse Power Law Model,"Phys. Rev. D **79**, 103004 (2009)

Harko, Tiberiu, Francisco SN Lobo, Shin'ichi Nojiri, and Sergei D. Odintsov. "f (R, T) gravity." Physical Review D 84, no. 2 (2011): 024020.

T. Harko,"Thermodynamic interpretation of the generalized gravity models with geometry - matter coupling,"Phys. Rev. D **90**, no.4, 044067 (2014)

L. K. Sharma, A. K. Yadav, P. K. Sahoo and B. K. Singh,"Non-minimal matter-geometry coupling in Bianchi I space-time,"Results Phys. **10**, 738-742 (2018)

A. K. Yadav, L. K. Sharma, B. K. Singh and P. K. Sahoo,"Existence of bulk viscous universe in $f(R,T)$ gravity and confrontation with observational data,"New Astron. **78**, 101382 (2020)

L. K. Sharma, A. K. Yadav and B. K. Singh, "Power-law solution for homogeneous and isotropic universe in $f(R,T)$ gravity,"New Astron. **79**, 101396 (2020)

L. K. Sharma, B. K. Singh and A. K. Yadav, "Viability of Bianchi type V universe in $f(R,T) = f_1(R) + f_2(R)f_3(T)$ gravity,"Int. J. Geom. Meth. Mod. Phys. **17**, no.07, 2050111 (2020)

S. Nojiri and S. D. Odintsov, "Unified cosmic history in modified gravity: from F(R) theory to Lorentz non-invariant models,"Phys. Rept. **505**, 59-144 (2011)

S. M. Carroll, V. Duvvuri, M. Trodden and M. S. Turner, "Is cosmic speed - up due to new gravitational physics?,"Phys. Rev. D **70**, 043528 (2004)

W. Hu and I. Sawicki,"Models of f(R) Cosmic Acceleration that Evade Solar-System Tests,"Phys. Rev. D **76**, 064004 (2007)

F. G. Alvarenga, A. de la Cruz-Dombriz, M. J. S. Houndjo, M. E. Rodrigues and D. Sáez-Gómez,"Dynamics of scalar perturbations in $f(R,T)$ gravity,"Phys. Rev. D **87**, no.10, 103526 (2013)

P. K. Sahoo, P. Sahoo and B. K. Bishi,"Anisotropic cosmological models in $f(R,T)$ gravity with variable deceleration parameter,"Int. J. Geom. Meth. Mod. Phys. **14**, no.06, 1750097 (2017)

Z. Yousaf, K. Bamba and M. Z. u. H. Bhatti,"Causes of Irregular Energy Density in $f(R,T)$ Gravity,"Phys. Rev. D **93**, no.12, 124048 (2016)

Z. Yousaf, M. Z. u. H. Bhatti and M. Ilyas, "Existence of compact structures in $f(R,T)$ gravity,"Eur. Phys. J. C **78**, no.4, 307 (2018)

Z. Yousaf, K. Bamba and M. Z. u. H. Bhatti, "Influence of Modification of Gravity on the Dynamics of Radiating Spherical Fluids,"Phys. Rev. D **93**, no.6, 064059 (2016)

Z. Yousaf, K. Bamba, M. Z. Bhatti and U. Ghafoor, "Charged Gravastars in Modified Gravity,"Phys. Rev. D **100**, no.2, 024062 (2019)

A. Das, F. Rahaman, B. K. Guha and S. Ray,"Compact stars in $f(R,\mathcal{T})$ gravity,"Eur. Phys. J. C **76**, no.12, 654 (2016)

A. K. Yadav, P. K. Sahoo and V. Bhardwaj,"Bulk viscous Bianchi-I embedded cosmological model in f(R,T) = f1(R) + f2(R)f3(T) gravity,"Mod. Phys. Lett. A **34**, no.19, 1950145 (2019)

This paper has been typeset from a TEX/LATEX file prepared by the author.